

# Assembly of a Gigantic Polyoxometalate Cluster $\{W_{200}Co_8O_{660}\}$ in a Networked Reactor System\*\*

Andreu Ruiz de la Oliva, Victor Sans, Haralampos N. Miras, Jun Yan, Hongying Zang, Craig J. Richmond, De-Liang Long, and Leroy Cronin\*

The field of polyoxometalates (POMs) is expanding rapidly owing to the highly configurable structures,<sup>[1]</sup> range of applications,<sup>[2]</sup> and deceptively complex universal one-pot reaction methods for the synthesis of these clusters.<sup>[3]</sup> However one important problem is that one-pot reactions mask a vast and complex range of intricate self-assembly processes that must invariably occur in solution, and it is therefore difficult to predict or control the assembly process. This issue is not limited to polyoxometalates, but extends to a vast number of other chemical systems such as supramolecular inorganic chemistry,<sup>[4]</sup> nanoparticles,<sup>[5]</sup> DCLs (dynamic combinatorial libraries),<sup>[6]</sup> and coordination chemistry.<sup>[7]</sup> One approach to systematically explore the systems could be to do multiple and combinatorial reactions one-by-one, but this only probes the combinatorial space in a very limited sense. However, the rapid screening and integration of a large number of one-pot reactions would be transformative since this would allow both compositional and time-dependent space to be integrated, and networked, yet this has never before been proposed or realized experimentally, see Figure 1.

Thus the development of a networked one-pot reaction array (Figure 1c) should be of fundamental importance since linking multiple complex assembly processes, such as those found in one-pot systems, provides potential not only for the reproducible assembly of complex nanostructures,<sup>[8]</sup> but also allows the systematic combination of one-pot reactions of similar systems as a function of time or composition permitting the exploration of virtual libraries of building blocks.<sup>[9]</sup> Potentially this could lead to the control of assembly at the molecular level by using macrocontrol in a series of one-pot reactions connected in a flow system.

Herein, we use a networked reactor system (NRS) for the discovery of polyoxometalate clusters. Specifically we applied this approach to the synthesis of an unknown family of metal-containing isopolyoxotungstates (iso-POTs) in the presence of templating transition metals such as  $Co^{2+}$  (Figure 2) by screening networks of one-pot reactions. This result shows

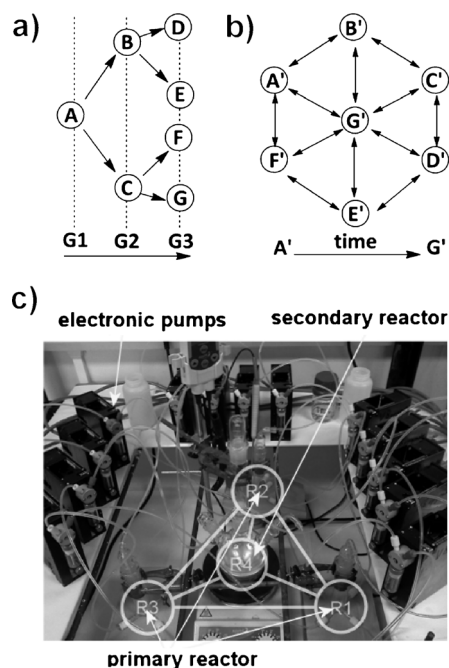


**Figure 1.** Top: comparison between conventional parameter space (a; i.e. generations G1, G2, and G3) and networked multiple parameter screenings (b), in X or X' one-pot reactions (where X = A to G). Bottom: photograph of the networked one-pot reactor array (c).

that the NRS approach can lead to the discovery of new clusters in a reproducible way and allows one-pot reactions to be probed or expanded over a number of reaction vessels, rather than relying on one single vessel. As such, the use of the NRS led to the discovery of a chain-linked iso-POT  $\{(DMAH)_6[H_4CoW_{11}O_{39}] \cdot 6H_2O\}_n$  ( $\{W_{11}Co\}_n$ ; **1**), a cobalt-trapped iso-POT  $Na_4(DMAH)_{10}[H_4CoW_{22}O_{76}(H_2O)_2] \cdot 20H_2O$  ( $\{W_{22}Co\}$ ; **2**) and,  $Na_{16}(DMAH)_{72}[H_{16}Co_8W_{200}O_{660} \cdot (H_2O)_{40}] \cdot ca.600H_2O$  ( $\{W_{200}Co_8\}$ ; **3**), which is over 4 nm in diameter and represents the largest discrete polyoxotungstate cluster so far characterized.<sup>[10]</sup> This cluster is formed uniquely in the NRS as several different one-pot reaction processes can be set up independently and mixed together leading to the interconnection of building blocks synthesized in the network of reactors, which are then linked to yield the final cluster compounds.

Discovery of the  $\{W_{200}Co_8\}$  is accomplished uniquely in the NRS; this result is interesting since it opens the way for nanoscale control by using macroscale parameters. This is because the NRS is designed to combine two aspects: the synthesis of new compounds by linking separate one-pot

[\*] A. R. de la Oliva, Dr. V. Sans, Dr. H. N. Miras, Dr. J. Yan, H. Zang, Dr. C. J. Richmond, Dr. D.-L. Long, Prof. L. Cronin  
WestCHEM, School of Chemistry, The University of Glasgow  
Glasgow G12 8QQ, Scotland (UK)  
E-mail: lee.cronin@glasgow.ac.uk  
Homepage: <http://www.croninlab.com>

[\*\*] We thank the EPSRC, WestCHEM, and the University of Glasgow for supporting this work.

Supporting information for this article is available on the WWW under <http://dx.doi.org/10.1002/anie.201206572>.

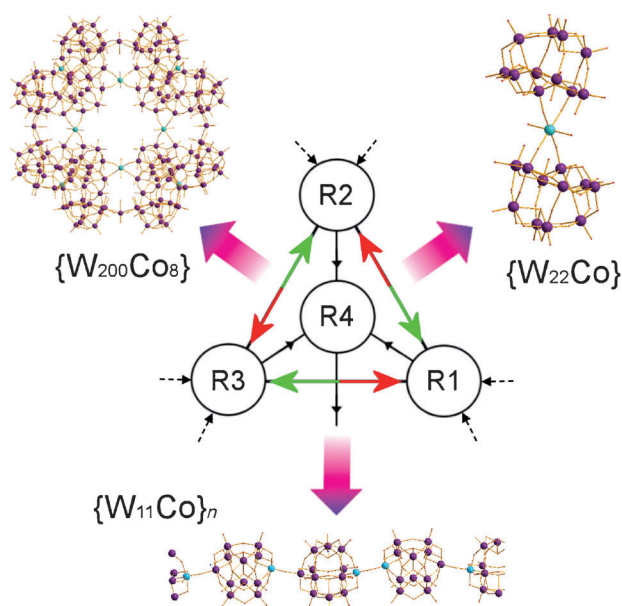


**Figure 2.** Schematic representation of the networked reactor system (red and green arrows show the clockwise and anticlockwise circulation of the one-pot reactions) and the new structures are highlighted around the triangular networked reactor system. Crystal structures of compounds **1**  $\{W_{11}Co\}_n$ , **2**  $\{W_{22}Co\}$ , and **3**  $\{W_{200}Co_8\}$  are shown in ball and stick mode. Colour scheme: W purple, Co cyan, O red.

reactions each containing unique building blocks (BBs), and then subsequent mixing of these individual one-pot reactions, that is, moving the reagents from reactor to reactor. Thus the NRS allows control of the reaction in both time and space (by comparison we consider that normal one-pot reactions only search in time). In the simple implementation of the NRS three primary reactors, each with two external reagent inputs, are connected together in a triangular arrangement with a central secondary reactor (connected to all three primary reactors; see Figure 2 and the Supporting Information). The NRS has a high connectivity, thus allowing a wide range of multiple mixing pathways in which the reagents can be moved from one flask to another (i.e. anticlockwise  $R1 \rightarrow R2 \rightarrow R3 \rightarrow R4$  or clockwise  $R1 \rightarrow R3 \rightarrow R2 \rightarrow R4$ , Figure 2). This flexibility allows recycling and refeeding processes according to  $(R1 \rightarrow R2 \rightarrow R3)_n$  ( $n$  = number of cycles) depending on standard flow parameters in the NRS. In contrast to a linear setup,<sup>[8]</sup> the NRS allows many different reagent inputs to be accommodated in separate reactors. Moreover, the system can allow both the screening and automation of the syntheses of a range of different clusters (e.g. compounds **1–3**) by selecting the reaction and flow parameters (flow rates, pH, initial volumes, etc.) in a highly automated, controlled, and reproducible manner.

The gigantic isopolyanion compound **3**,  $\{W_{200}Co_8\}$ , has a saddle-shaped structure,<sup>[11]</sup> contains unusual pentagonal units, and crystallizes as a hydrate sodium and dimethylammonium salt of  $[H_{16}Co_8W_{200}O_{660}(H_2O)_{40}]^{88-}$ . Single crystal X-ray diffraction shows that the crystals have a tetragonal structure with space group  $P4_2/nmc$ . The cluster itself has an approximate  $D_{2d}$  symmetry and the building blocks are shown in Figure 3.

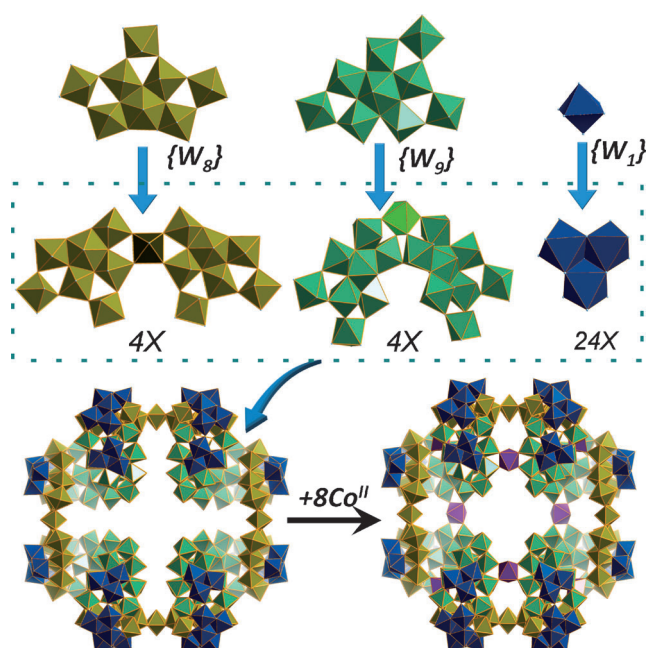


**Figure 3.** Representation of the crystal structure of compound **3**. The three principal building blocks are represented at the top, where  $\{W_8\}$  and  $\{W_9\}$  are derived from  $\{W(W)_3\}$  pentagonal units. The secondary building blocks are represented in the middle section, and are formed as a result of condensation of the principal building blocks. The synthesis of compound **3** is completed by the complexation of 8 cobalt ions (purple).

The building unit of this cluster (**3**) is fundamentally different from the classic isopolyoxotungstates,<sup>[12a]</sup> for example, those found in the  $\{W_{36}\}$  cluster.<sup>[12b]</sup> Instead the  $\{W_{200}Co_8\}$  cluster presented here comprises three types of principal building blocks (PBBs):  $\{W_1\}$ ,  $\{W_8\}$ , and  $\{W_9\}$  derived from  $\{WO_7\}$ -centered bipentagonal building blocks, whereby the  $\{W_9\}$  contains a complete  $\{W(W)_5\}$  pentagonal fragment and the  $\{W_8\}$  contains a  $\{W(W)_4\}$  pentagonal unit with a defect position. It is interesting that such pentagonal units were first observed in the mixed valence molybdate blue/brown family and are considered to be key units for the construction of these POM clusters.<sup>[9]</sup> As with the molybdate analogues, the  $\{WO_7\}$  units are formed and captured owing to the reduction of the tungsten centers, but their further assembly is different because the tungsten centers are quickly reoxidised within the NRS one-pot network array. Structurally speaking, two  $\{W_8\}$  units are condensed and linked up by a  $\{W_1\}$  unit in a *trans* mode and the resulting secondary building block (SBB) consists of 15 W sites including two pentagonal  $\{WO_7\}$  units. The two relevant  $\{W(W)_4\}$  planar units are linked with a dihedral angle of  $26.61(1)^\circ$ . In contrast, two  $\{W_9\}$  PBB units are condensed to form a  $\{W_{17}\}$  SBB and linked up in a *cis* mode, which leads to a more-twisted SBB containing the two  $\{W(W)_5\}$  planar units crossed with a dihedral angle of  $31.20(1)^\circ$ . Four  $\{W_{15}\}$  and four  $\{W_{17}\}$  SBBs connect alternately to each other through a shared oxo ligand and form the main body of the cluster. Furthermore, the planar pentagonal sites have a structure that is good for binding the  $\{W_3\}$  SBBs, which always exist in acidic tungstate solution, so that 16  $\{W_3\}$  units are added to the side of these pentagonal units. Remarkably,

the  $\{W_3\}$  unit has all the terminal oxo ligands oriented towards one side; this makes it a good stopper ligand and eight more  $\{W_3\}$  SBB units are located on the surface of the cluster, these units effectively prevent the cluster from linking to form an infinite network or a system larger than the discrete  $\{W_{200}Co_8\}$  system. Nevertheless, the eight captured cobalt ions also play an important role, not only for charge balancing reasons but also for stabilizing the SBB units such as  $\{W_9\}$ . Four cobalt ions link the four  $\{W_{17}\}$  SBBs through corner-sharing oxo ligands; structurally the  $\{W_9Co\}$  is very similar to the  $\{Mo_{10}\}$  SBB units found in the gigantic the  $\{Mo_{154}\}$  ring cluster.<sup>[13]</sup>

By designing the experiments in the NRS, the approach is divided into three ( $R1 \rightarrow R2 \rightarrow R3$ )<sub>n</sub> phases: a first phase allows the introduction of reagents and a second phase is used to adjust local parameters such as pH or ionic strength/cation type. This allows the discrete formation of different building blocks in each individual reactor. A third phase allows the introduction of the  $Na_2S_2O_4$  reducing agent and the cobalt chloride transition metal salt in reactors R2 and R3, respectively (see Figure 4).

The pH control in each of the reactors is important since it allows a set building blocks consisting of a  $\{W_{12}\}$ -Keggin, a flatter  $\{W_{12}\}$ , and a  $\{W_{11}\}$  to be generated in a controlled way<sup>[14]</sup> because  $\{W_{12}\}$  forms at  $pH > 4$  and  $\{W_{11}\}$  at lower pH.<sup>[15]</sup> Additionally, the  $\{W_{12}\}$  building block clusters may be rearranged easily to lacunary Keggin-like structures when the pH is increased.<sup>[16]</sup> Thus, the assembly of compounds 1–3 is defined by mixing different  $\{W_{11}\}$ ,  $\{W_{12}\}$ , and  $\{Co-W_x\}$  clusters in the second and third phases (see Figure 5). The local pH values, such as  $pH_{R1} < pH_{R2} < pH_{R3}$ , can be controlled by addition of the reagents, and both the pH and UV/Vis can be monitored simultaneously in reactors R1, R2, and R3. These studies confirm that the reaction conditions are suitable for the formation of  $\{W_{11}\}$  and  $\{W_{12}\}$  only after the pH drops. Then the  $Na_2S_2O_4$  and cobalt chloride salt were added dropwise separately to R2 and R3, respectively, just after BBs were created while recycling to yield such compounds 1–3. This third phase is particularly interesting because a template–BB interaction is taking place at a controlled flow rate. The pH values change during this third and last phase as the  $Na_2S_2O_4$  solution provides basicity in R2 and the  $CoCl_2$  solution dilutes R3. The pH was monitored until all the reagents had reached R4 by  $R1 \rightarrow R4$  (1 at  $pH_{R4} = 4.2$ , 2 at  $pH_{R4} = 3.6$  and, finally, 3 at  $pH_{R4} = 2.5$ ); the reaction mixture

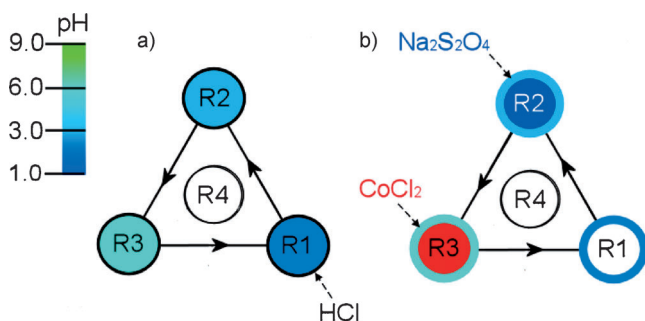


**Figure 4.** Space- and time-dependent NRS approach for the synthesis of  $\{W_{200}Co_8\}$  (3). The different pH values are shown for the primary reactors during the last stages of the second recycling process (a) and initial stages of the refeeding process (b).

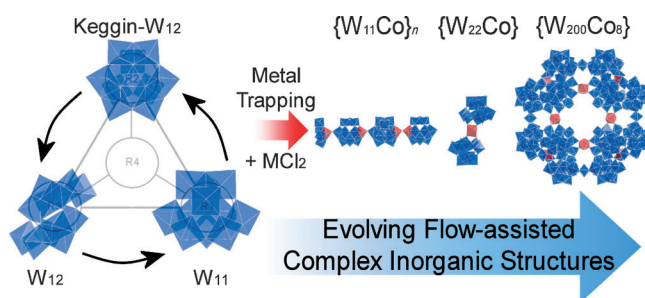


**Figure 5.** General scheme for the space- and time-dependent NRS approach, showing the distribution of the different isotungstates in the primary reactors to give to different final template–BB interactions and different final products:  $\{W_{11}Co\}_n$ ,  $\{W_{22}Co\}$ , and  $\{W_{200}Co_8\}$ . W blue, Co red.

was stirred in R4 for 15 min. In addition to the pH monitoring, the in situ recording of UV/Vis spectra individually for R1, R2, and R3 gives further information about the assembly as the absorption bands for oxo-tungstate(VI) based BBs show an intense band between 300 and 400 nm (see the Supporting Information).<sup>[17]</sup>

In this work, the self-assembly processes are controlled by modulation of the reaction conditions, thus allowing different libraries of building blocks from each of the reactors (R1, R2, and R3) to be condensed together within the NRS. In terms of BBs, the explanation for the formation of compound 1 is that the formation of monolacunary-Keggin- $\{W_{11}\}$  is favored because the working pH range facilitates an easy rearrangement to Keggin-like structures. In contrast, for compound 2 the working pH is lower, stabilizing the  $\{W_{11}\}$  subunits under reducing conditions by coordination to  $\{Co(H_2O)_6\}^{2+}$  centers, as observed previously.<sup>[12]</sup> Furthermore, the discovery of eight cobalt-trapped cluster isopolyanions  $\{H_{16}W_{200}Co_8O_{660}(H_2O)_{40}\}^{88-}$  in compound 3 is important from a structural point of view because the cluster is formed from an unexpected tungstate building-block library (PBB and SBB) by multi-cobalt-trapping self-assembly. These results demonstrate the potential of the NRS to allow the synthesis and combination of fundamentally different building blocks, as well as allowing new architectures to be isolated by the introduction of the metal centers into the NRS.

In conclusion, for the first time, a networked reactor system (NRS) is presented wherein multiple one-pot connected reactions are screened, the reaction variables explored, and automation of the syntheses of the compounds 1, 2, and 3 achieved. The potential of the NRS methodology is transformative owing to the ability to explore one-pot reactions as configurable modules, and to explore different mixing and reaction conditions in a programmed and sequential way (stepwise process) as well as allowing the combination of building block libraries that could not coexist in classical one-pot reactions. This is because the NRS allows the combination of pH adjustment and UV monitoring in real time, thus controlling different local experimental conditions in each reactor within the system. This feature makes the NRS potentially very useful to explore other combinations of initial reagents, to study reaction mechanisms and self-assembly reactions in other areas of chemistry (i.e. coordination



chemistry or design of metal–organic frameworks). As such, we demonstrate macroscale control of the assembly of polyoxometalates for the first time, and this builds on our observations of microscale<sup>[19]</sup> control of assembly and opens opportunities to utilize the approach shown here in exploring the assembly of new inorganic structures in the NRS, for instance, polyoxometalates with high nuclearity and charge.

## Experimental Section

**Synthesis of compounds 1–3:** The aqueous stock solutions (50 mL) were prepared as follows: Solution A: 2.8 M Na<sub>2</sub>WO<sub>4</sub>·2H<sub>2</sub>O (6.7 mL; 6.19 g, 19 mmol). Solution B: 2.0 M DMA·HCl (31 mL; 5.06 g, 62 mmol). Solution C: 0.5 M Na<sub>2</sub>S<sub>2</sub>O<sub>4</sub> (3.6 mL; 0.31 g, 1.8 mmol). Solution D: 0.5 M CoCl<sub>2</sub>·6H<sub>2</sub>O (2.1 mL; 0.25 g, 1.1 mmol). Solution E: 6 M HCl (2.9 mL for **1**, 3.3 mL for **2** and 4.0 mL for **3**). All experiments were carried out using the following general method: The stock solutions of reagents were connected to the inlets for the assigned pumps. The prewritten matrix commands were then executed to initiate the pumping. Solution A is added into reactor R3, solution B into reactor R2, and an extra amount of water (7 mL) into reactor R1. These solutions are mixed at an average of 7 mL min<sup>−1</sup> in proper volume proportions (V<sub>R1</sub>/V<sub>R2</sub>/V<sub>R3</sub>) and started to flow around the primary sector within channels connecting reactors R1, R2, and R3. At the same time, solution E is added in R1 until a desired pH value pattern is obtained in the primary sector. Then, solutions C and D are added dropwise while the third phase is taking place. During this process, initially the solution is getting darker in R2 and red in R3, and afterwards all solutions in the primary sector become a darker blue. The solution is pumped from the primary sector to the R4 where it is stirred for 15 min. The final solution is collected in a 100 mL open flask and allowed to crystallize (1 week for **1**, 1 month for **2**, and 2 months for **3**).

Crystal data and structure refinements for following compounds: {(DMAH)<sub>6</sub>[H<sub>4</sub>CoW<sub>11</sub>O<sub>39</sub>]·6H<sub>2</sub>O}<sub>n</sub> (**1**): C<sub>12</sub>H<sub>64</sub>Co<sub>6</sub>N<sub>6</sub>O<sub>45</sub>W<sub>11</sub>, M<sub>r</sub> = 3093.97 g mol<sup>−1</sup>; dark-purple long crystal. Orthorhombic; space group *Cmca*, *a* = 20.8174(6), *b* = 26.7054(6), *c* = 21.7302(6) Å; V = 12080.6(6) Å<sup>3</sup>; Z = 8; ρ = 3.402 g cm<sup>−3</sup>; λ(Mo-Kα) = 0.71073 Å; 47723 reflections measured; 5917 unique reflections (R<sub>int</sub> = 0.0715) which were used in all calculations; 361 refined parameters; final R1 = 0.0533 and wR2 = 0.1197 (all data).

Na<sub>4</sub>(DMAH)<sub>10</sub>[H<sub>4</sub>CoW<sub>22</sub>O<sub>76</sub>(H<sub>2</sub>O)<sub>2</sub>]·20H<sub>2</sub>O (**2**): C<sub>20</sub>H<sub>128</sub>Co<sub>10</sub>N<sub>10</sub>Na<sub>4</sub>O<sub>98</sub>W<sub>22</sub>, M<sub>r</sub> = 6272.91 g mol<sup>−1</sup>; pink needle-shaped crystal. Triclinic; space group *P* $\bar{1}$ , *a* = 12.2125(4), *b* = 14.7989(4), *c* = 17.2296(5) Å; α = 92.450(1)°, β = 108.331(1)°, γ = 103.469(1)°; V = 2851.83(15) Å<sup>3</sup>; Z = 1; ρ = 3.653 g cm<sup>−3</sup>; λ(Mo-Kα) = 0.71073 Å; 41327 reflections measured; 11212 unique reflections (R<sub>int</sub> = 0.0261) which were used in all calculations; 694 refined parameters; final R1 = 0.0226 and wR2 = 0.0607 (all data).

Na<sub>16</sub>(DMAH)<sub>72</sub>[H<sub>16</sub>Co<sub>8</sub>W<sub>200</sub>O<sub>660</sub>(H<sub>2</sub>O)<sub>40</sub>]·ca. 600H<sub>2</sub>O (**3**): C<sub>144</sub>H<sub>1872</sub>Co<sub>8</sub>N<sub>72</sub>Na<sub>16</sub>O<sub>1300</sub>W<sub>200</sub>, M<sub>r</sub> = 63034.4 g mol<sup>−1</sup>; light pink needle-shaped crystal. Tetragonal; space group *P*4<sub>2</sub>/nmc, *a* = 48.5465(12), *c* = 29.4217(10) Å; V = 69340(3) Å<sup>3</sup>; Z = 2; ρ = 3.019 g cm<sup>−3</sup>; λ(Mo-Kα) = 0.71073; 465910 reflections measured; 31284 unique reflections (R<sub>int</sub> = 0.1215) which were used in all calculations; 1419 refined parameters; final R1 = 0.0867 and wR2 = 0.2791 (all data). Data collection and reduction were performed using the CrysAlis software package and structure solution and refinement were carried out using SHELXS-97 and SHELXL-97. Corrections for incident and diffracted beam absorption effects were applied using empirical absorption correction. CCDC 895469 (**1**), 895470 (**2**) and 895471 (**3**) contain the supplementary crystallographic data for this paper. These data can be obtained free of charge from The Cambridge Crystallographic Data Centre via [www.ccdc.cam.ac.uk/data\\_request/cif](http://www.ccdc.cam.ac.uk/data_request/cif).

Received: August 15, 2012

Published online: November 23, 2012

**Keywords:** networked reaction system · one-pot reactions · polyoxometalates · polyoxotungstates · self-assembly

- [1] a) D.-L. Long, E. Burkholder, L. Cronin, *Chem. Soc. Rev.* **2007**, 36, 105–121; b) D.-L. Long, L. Cronin, *Chem. Eur. J.* **2006**, 12, 3698–3706.
- [2] a) D. G. Kurth, *Sci. Technol. Adv. Mater.* **2008**, 9, 014103; b) I. Ichinose, T. Kunitake, *Chem. Rec.* **2002**, 2, 339–351; c) L. Lisnard, A. Dolbecq, P. Mialane, J. Marrot, E. Codjovi, F. Sécheresse, *Dalton Trans.* **2005**, 3913–3920; d) M. I. Khan, *J. Solid State Chem.* **2000**, 152, 105–112; e) S. Liu, Z. Tang, *Nano Today* **2010**, 5, 267–281; f) A. R. Gaspar, J. A. F. Gamelas, D. V. Evtuguin, C. P. Neto, *Green Chem.* **2007**, 9, 717–730; g) J. T. Rhule, C. L. Hill, D. A. Judd, *Chem. Rev.* **1998**, 98, 327–357; h) W. Qi, L. Wu, *Polym. Int.* **2009**, 58, 1217–1225; i) D. Sloboda-Rozner, P. Witte, P. L. Alster, R. Neumann, *Adv. Synth. Catal.* **2004**, 346, 339–345.
- [3] a) D.-L. Long, R. Tsunashima, L. Cronin, *Angew. Chem.* **2010**, 122, 1780–1803; *Angew. Chem. Int. Ed.* **2010**, 49, 1736–1758; b) C. P. Pradeep, D.-L. Long, L. Cronin, *Dalton Trans.* **2010**, 39, 9443–9457; c) H. N. Miras, J. Yan, D.-L. Long, L. Cronin, *Chem. Soc. Rev.* **2012**, 41, 7403–7430.
- [4] X. Fang, P. Kögerler, Y. Furukawa, M. Speldrich, M. Luban, *Angew. Chem.* **2011**, 123, 5318–5322; *Angew. Chem. Int. Ed.* **2011**, 50, 5212–5216.
- [5] S. Marre, K. E. Jensen, *Chem. Soc. Rev.* **2010**, 39, 1183–1202.
- [6] R. A. R. Hunt, S. Otto, *Chem. Commun.* **2011**, 47, 847–858.
- [7] V. E. Campbell, X. de Hatten, N. Delsuc, B. Kauffmann, I. Huc, J. R. Nitschke, *Nat. Chem.* **2010**, 2, 684–687.
- [8] a) H. N. Miras, G. J. T. Cooper, D.-L. Long, H. Bögge, A. Müller, C. Streb, L. Cronin, *Science* **2010**, 327, 72–74; b) H. N. Miras, C. J. Richmond, D.-L. Long, L. Cronin, *J. Am. Chem. Soc.* **2012**, 134, 3816–3824.
- [9] A. Müller, P. Kögerler, C. Kuhlmann, *Chem. Commun.* **1999**, 1347–1358.
- [10] a) K. Wassermann, M. H. Dickman, M. T. Pope, *Angew. Chem.* **1997**, 109, 1513–1516; *Angew. Chem. Int. Ed. Engl.* **1997**, 36, 1445–1448; b) F. Hussain, G. R. Patzke, *CrystEngComm* **2011**, 13, 530–536.
- [11] J. Yan, J. Gao, D.-L. Long, H. N. Miras, L. Cronin, *J. Am. Chem. Soc.* **2010**, 132, 11410–11411.
- [12] a) H. N. Miras, J. Yan, D.-L. Long, L. Cronin, *Angew. Chem.* **2008**, 120, 8548–8551; *Angew. Chem. Int. Ed.* **2008**, 47, 8420–8423; b) D.-L. Long, H. Abbas, P. Kögerler, L. Cronin, *J. Am. Chem. Soc.* **2004**, 126, 13880–13881.
- [13] A. Müller, E. Krickemeyer, J. Meyer, H. Bögge, F. Peters, W. Plass, E. Diemann, S. Dillinger, F. Nonnenbruch, M. Randerath, M. Carsten, *Angew. Chem.* **1995**, 107, 2293–2295; *Angew. Chem. Int. Ed. Engl.* **1995**, 34, 2122–2124.
- [14] A. Chrissafidou, J. Fuchs, H. Hartl, R. Palm, *Z. Naturforsch. B* **1995**, 50, 217–222.
- [15] T. Lehmann, J. Fuchs, *Z. Naturforsch. B* **1988**, 43, 89–93.
- [16] I. A. Weinstock, J. J. Cowan, E. M. G. Barbuzzi, H. Zeng, C. L. Hill, *J. Am. Chem. Soc.* **1999**, 121, 4608–4617.
- [17] D. Ravelli, D. Dondi, M. Fagnoni, A. Albini, A. Bagno, *J. Comput. Chem.* **2011**, 32, 2983–2987.
- [18] X. Zhuang, G. Su, Y. He, G. Zheng, *Cryst. Res. Technol.* **2006**, 41, 1031–1035.
- [19] G. J. T. Cooper, R. W. Bowman, E. P. Magennis, F. Fernandez-Trillo, C. Alexander, M. J. Padgett, L. Cronin, *Angew. Chem.* **2012**, DOI: 10.1002/ange.201204405; *Angew. Chem. Int. Ed.* **2012**, DOI: 10.1002/anie.201204405.